T H E U N I V E R S I T Y O F M I C H I G A N
COLLEGE OF ENGINEERING
Department of Electrical Engineering
Space Physics Research Laboratory

Technical Report No. 2

THE ACOUSTIC WIND MEASUREMENT

W. W. Bushman
G. M. Kakli
M. E. Graves

ORA Project 07871

Under contract with:

NATIONAL AERONAUTICS AND SPACE ADMINISTRATION
GEORGE C. MARSHALL SPACE FLIGHT CENTER
CONTRACT NO. NAS8-20357
HUNTSVILLE, ALABAMA

Administered through:

OFFICE OF RESEARCH ADMINISTRATION ANN ARBOR

Feb. 1968

Introduction

This report discusses contractual effort for the period March to December 1967 on Contract number NAS8-20357. This effort was concentrated in four areas of the acoustic wind measuring technique.

The first area, the analysis of errors from past flights and the recomputation of wind profiles based on this analysis was plagued by computer problems and required the entire reporting period to complete. This work is characterized by a series of steps each depending on computed results from a prior step and was frequently interrupted by computer breakdowns. Results and descriptions of this analysis are presented in another section.

Another area of work is the study of atmospheric tides. A description of this study is also available in another section of this report.

A third effort, aimed at deriving vertical winds or temperature profiles from the acoustic data has not yet yielded satisfactory results. This technique, based on equations published by Groves* suffers from a lack of compatibility between the measurement precision, the microphone spacing, and typical distances to the sound source. This method might be productive if microphone spacing is increased. To test this hypothesis, raw, far field, acoustic

*Journal of Atmospheric and Terrestrial Physics, Vol. 7, pp. 113-127.
Journal of Atmospheric and Terrestrial Physics, Vol. 8, pp. 24-36.
Journal of Atmospheric and Terrestrial Physics, Vol. 8, pp. 189-203.

data from Apollo 4 has been requested. However, while the microphone spacing in these measurements is improved (3 - 6 miles) it may be impossible to cross correlate the data to determine arrival times. These possibilities will be evaluated when the acoustic data are received.

An opportunity to check the possibility of reducing the scatter in time difference by using the higher frequencies of the acoustic spectrum became available during the launch of Apollo 4. Mr. Andrew Thompson from the Ballistic Research Laboratory monitored the Apollo 4 launch with 3 wide band sensors manufactured by Globe Exploration Company of El Paso, Texas. These sensors were set up in a southbound line starting near microphone No. 4. The separation between adjacent microphones was approximately 300 feet but these locations were not surveyed. The output of each microphone was passed through a voltage divider and the reduced and full scale outputs were both recorded. Thus data for a total of 6 sensitivities was collected on 6 channels of a magnetic tape. Mr. Thompson graciously made available copies of the recorded data.

Two of the six channels were chosen for study because the sensitivities differed only by a factor of 2 and both yielded about 100 seconds of valid data. These data came from the two end microphones, a separation of about 600 feet, which is not much different from the hot wire microphone separation. Cross correlations were computed and time differences plotted. The initial results indicate that no improvement in accuracy can be expected by using

acoustic data from the higher frequencies. However, time difference scatter from the hot wire microphones for this flight has not yet been determined and this information may reverse this conclusion.

Tidal Motion in the Atmosphere

Maurice E. Graves

Introduction

The acoustic wind measurements at Cape Kennedy have various secondary effects incorporated within the data which alter the irregular dynamic flow patterns over the station. These effects include thermally-excited tides of two or more detectable periods, internal gravity waves, turbulence, and external gravitational influences. Of these four phenomena, the thermal tides are believed to attain the largest amplitude of wave motion; hence, the derivation of suitable formulas for tidal winds at Cape Kennedy at any given time is of great interest. A complete summary of work in this field prior to 1961 was written by Siebert [1], and some outstanding papers have been published by Lindzen [2,3,4] since 1965.

Barograms obtained at the ground reveal a diurnal thermal tide with the first three harmonics, plus a semidiurnal lunar tide. The semidiurnal, solar, thermal tide is by far the most conspicuous of these waves, and the explanation of this has posed a problem to theoreticians. A currently accepted view is that the diurnal, thermal tide is suppressed in the lower troposphere, thus masking its importance at higher levels. The alternative, which enjoyed much support in former years, is that the remarkable 12-hour ground pressure wave is due to resonance magnification in the atmosphere with a free period nearer 12 hours than 24 hours.

J_n = thermal forcing function, n^{th} mode

In this derivation, only periodic processes are considered, so that

$$u', v', w', \chi, J \propto e^{i\omega t} \tag{2}$$

u' = tidal west wind

v' = tidal north wind

w' = tidal vertical velocity

ω = angular frequency of oscillation

t = time

s = longitudinal wave number = 1

λ = longitude

Expressions for the Tidal Winds

For the diurnal tide, $\omega = \Omega$, where Ω = angular speed of Earth's rotation. In terms of the transformed variables y and x, the tidal winds can now be expressed [4] in terms of the n^{th} mode.

$$u_n' = \frac{i\gamma g h_n}{4a\Omega^2} e^{\frac{x}{2}} \left(y_n' - \frac{y_n}{2}\right) \frac{1}{(f^2-\mu^2)} \left(\frac{\cos\phi}{f}\frac{\partial}{\partial\phi} - \frac{i}{\sin\phi}\frac{\partial}{\partial\lambda}\right)\left[\Theta_n e^{i(\omega t+s\lambda)}\right] \tag{3}$$

$$v_n' = \frac{\gamma g h_n}{4a\Omega^2} e^{\frac{x}{2}} \left(y_n' - \frac{y_n}{2}\right) \frac{1}{(f^2-\mu^2)} \left(\frac{\partial}{\partial\phi} - \frac{i}{f}\cot\phi\frac{\partial}{\partial\lambda}\right)\left[\Theta_n e^{i(\omega t+s\lambda)}\right] \tag{4}$$

$$w_n' = \gamma h_n e^{\frac{x}{2}} \left[y_n' + \left(\frac{H}{h_n} - \frac{1}{2}\right) y_n\right] \Theta e^{i(\omega t+s\lambda)} \tag{5}$$

$$\gamma = \frac{c_p}{c_v} = 1.4$$

a = radius of earth

Derivation of the "Radial Equation"

The classical derivation of the tidal wind equations assumes a dry atmosphere, no friction, the undisturbed elements temperature (T) and pressure (P) as functions of height (z), only, no vertical accelerations, and the validity of the Gas Law. It also assumes the Earth is a perfect sphere, rotating uniformly with angular velocity Ω. Then from the Euler Equations of Motion, the Continuity Equation, and the First Law of Thermodynamics, an expression for the 3-dimensional wind divergence is obtained by a perturbation technique [1]. In its final form, this expression is of second order, and functions of latitude, longitude, and height are all incorporated within it. By the method of separation of variables, it is resolved into a "Radial Equation", with height as the independent variable, and a "Laplace Tidal Equation", with latitude and longitude as the independent variables. A suitable transformation of height and divergence parameters yields a new "Radial Equation" for the n^{th} mode,

$$\frac{d^2 y_n(x)}{dx^2} - \frac{1}{4}\left[1 - \frac{4}{h_n}\left(\kappa H(x) + \frac{dH(x)}{dx}\right)\right] y_n(x) = \frac{\kappa}{g\gamma h_n} J_n(x) e^{-\frac{x}{2}} \qquad (1)$$

x = transformed height parameter $= \int_0^z \frac{d\zeta}{H(\zeta)}$

H = scale height

$y_n = \left[\chi_n(z) - \frac{\kappa}{g}\frac{J_n(z)}{H(z)}\right] e^{-\frac{x}{2}}$

χ_n = divergence of the wind, n^{th} mode

$\kappa = \frac{c_p - c_v}{c_p} = \frac{2}{7}$

g = gravity

$f = \omega/2\Omega$

$\mu = \cos \phi$

ϕ = colatitude, with $\phi = 0^{o}$ at N. Pole

λ = longitude

Ⓗ = Hough function, an eigensolution of the Laplace Tidal Equation

h_n = equivalent depth

$y_n = y_n(x)$

$y'_n = \frac{dy_n(x)}{dx}$

The factors in which Ⓗ, f, μ, ϕ and λ appear are all related to the Laplace Tidal Equation, and are given explicitly in graphical form for the 5 most important modes in [4]. Two of these modes are negative, corresponding to negative equivalent depths. This is a recent, major advance in the field of tidal theory [Lindzen, op. cit.] Then must be evaluated by solving (1), and the form of the solution depends upon the choice of $J_n(x)$. Following Lindzen [4] again, the thermal forces are assumed to be water vapor and ozone absorption, so that

$$J_n(H_2O) = \frac{i\omega R}{\kappa} e^{-\frac{x}{3}} e^{i(\omega t+s\lambda)} c_n \text{Ⓗ}_n \qquad (6)$$

$$J_n(O_3) = \frac{i\omega R}{\kappa} e^{0.0116(z-z_1)} \sin\left[\frac{\pi}{60}(z-z_1)\right] e^{i(\omega t+s\lambda)} c'_n \text{Ⓗ}_n \qquad (7)$$

The ozone effect is limited to 18-78 km and the c_n and c'_n are known constants.

Application to the Acoustic Wind Measurements

The particular solution of (1) is evidently of the form

$$y_n^* = Ae^{-\frac{5x}{6}} + \left(\frac{B}{\delta}\sin\tau + \frac{C}{\delta}\cos\tau\right)e^{(0.0116H-0.5)x} \qquad (8)$$

In obtaining this expression, the scale height is assumed constant and the longitudinal variation is dropped wherever it occurs in the exponential factor $e^{i(\omega t+s\phi)}$. A, B, C, δ and all vary with h_n and the first three of these also vary with Θ_n. In addition to (8), there is a term to be realized from the homogeneous part of (1) under certain boundary conditions. This term is complex for both negative and positive modes, as is the y^* in each case. The resulting y_n and y_n' give a rather complicated set of equations representing Eqs. (3) to (5). They are suitable for computer programing to obtain the diurnal tidal winds at numerous height levels for a particular time and latitude. The initial step taken was to find the tidal winds at 0600, 1200, 1800, and 2400 hours at Cape Kennedy and to compare them Lindzen's values at 30° Lat. [4]. The results are similar in some respects, but not entirely satisfactory with respect to the amplitude and phase of the fluctuations. Efforts are continuing to gain better agreement between the corresponding profiles.

In low latitudes, the magnitude of the theoretical wind tides above 90 km height are of the order of 100 m/sec, and near the tops of the highest acoustic soundings reported by Bushman [5], the horizontal tides are 30 - 40 m/sec and the vertical motion is about 5 cm/sec, in theory. Observational verification of the tidal winds below 60 km near 30° Lat. is fairly good when a large number of rocket soundings are subjected to harmonic analysis, as was done by Reed, McKenzie and Vyverberg [6]. On the other hand, radio-meteor observations in quantity by Elford [7] at 35°S. yielded somewhat smaller tidal winds than the theoretical estimates at the base of the

thermosphere. Observational data within the mesosphere above 60 km are almost completely absent, making the acoustic wind soundings a principal source of information in this layer for the testing of the tidal wind theory for horizontal motion.

References cited above:

1) Siebert, M., "Atmospheric Tides," Advances in Geophysics, 7, Academic Press, 1961, 105 - 182.

2) Lindzen, R. S., "On the Asymmetric Diurnal Tide", Pure and Applied Geophysics, 62, 1965, 142 - 147.

3) Lindzen, R. S., "On the Theory of the Diurnal Tide", Monthly Weather Review, 94, May 1966, 295 - 301.

4) Lindzen, R. S., "Thermally Driven Diurnal Tide in the Atmosphere," Quart, Journ. R. M. S. 93, Jan 1967, 18 - 42.

5) Bushman, W. W., "The Acoustic Wind Measurement: A Six Month Summary," Univ. of Mich. Tech. Report 07871-1-T, Sept. 1966.

6) Reed, R. J., McKenzie, D. J. and Vyverberg, J. C., "Further Evidence of Enhanced Diurnal Tidal Motions near the Stratopause," Journ. Atmos. Sci., 22, Mar. 1966, 247.

7) Elford, W. G., "A Study of Winds between 80 and 100 km in Medium Latitudes," Planet. Space Sci., 1, April 1959, 94 - 101.

ERRORS

G. M. Kakli & W. W. Bushman

It has been shown[1] that wind profile errors are caused, largely, by uncertainties in the microphone arrival time differences. Therefore the contribution of other sources of error are neglected in this section.

The procedure presently used to determine the time differences, described in detail in an earlier report[2] will be briefly outlined here.

The analogue magnetic tape recording of the microphone outputs and range time data is played through an A-D converter and recorded in digital form onto a magnetic tape. The sampling rate is 1000 samples/sec. channel. The cross correlation, R, is computed as follows:

$$R = \frac{\sum_{i=1}^{N} u_i v_i - \frac{\sum_{i=1}^{N} u_i \sum_{i=1}^{N} v_i}{N}}{\left\{\left(\sum_{i=1}^{N} u_i^2 - \frac{\left(\sum_{i=1}^{N} u_i\right)^2}{N}\right)\left(\sum_{i=1}^{N} v_i^2 - \frac{\left(\sum_{i=1}^{N} v_i\right)^2}{N}\right)\right\}^{1/2}}$$

where u_i and v_i represent samples of two microphone outputs (with mean value removed) and N is the number of sample pairs. These computations are performed for a pre-set data time interval usually .5 sec., so N = 500 sample pairs. The time at which R is maximum is taken to be the microphone arrival time difference.

To speed the cross correlation computation periodic rough estimates of expected time differences are also put into the program. These estimates are in turn based upon estimates of the sound source position as a function of range time. The computer then does not have to search over perhaps 2 seconds of data to find the principal maximum of R. The search can be restricted to 20-50 ms around the initial estimate depending upon the accuracy of the initial estimate. These limits of the search define a time interval called the tolerance.

Figure 1 is a plot of time difference between each microphone and microphone No. 1 as a function of range time. The scatter in the data shown in this figure, and its increase with range time is typical of all flights. As mentioned at the beginning of this section, the uncertainty in arrival time differences caused by this scatter is the major contributor to wind profile errors. The remainder of this section will describe how this uncertainty is related to characteristic velocity error and then how the characteristic velocity error is used to estimate wind profile errors.

The scatter in time is taken to be distributed randomly and described by a Gaussian (normal) distribution. This assumption is believed to be valid as long as the condition

$$\text{tolerance} >> \text{standard deviation } (\sigma)$$

is satisfied.

A straight line, $D = aT + b$ is fit over n data points, $\{(D_1,T_1), (D_2,T_2)\ldots(D_n,T_n)\}$ for each microphone.

Here D_k are time differences

T_k are range times

and a, b are constants determined by the least squares method. The n data points span a time interval which is initially taken to be 10 seconds and so there are a total of 21 data points in this interval. The time given by the straight line at the mid point of the interval, $\hat{D}$, is used for further calculations.

The standard estimate of error from the fitted line, σ_i, calculated for each microphone i, is

$$\sigma_i = \sqrt{\sum_{k=1}^{n} (D_k - aT_k - b)^2 \Big/ (n-2)}$$

The quantities Q_x and Q_y are defined as

$$Q_x = \frac{1}{4} \sum_{\{i\}} \frac{\hat{D}_i}{x_i} \qquad \{i\} = 4,5,6,7$$

(microphone numbering on x axis)

$$Q_y = \frac{1}{4} \sum_{\{i\}} \frac{\hat{D}_i}{y_i} \qquad \{i\} = 2,3,8,9$$

(microphone numbering on y axis)

Here x_i and y_i are the horizontal coordinates of the ith microphone.

The characteristic velocities K_x and K_y are

$$K_x = 1/Q_x$$

$$K_y = 1/Q_y$$

and the errors in Q's are

$$\Delta Q_x = \frac{t}{4}\sqrt{\sum_{\{i\}} \frac{\sigma_i^2}{n x_i^2}} \quad \{i\} = 4,5,6,7$$

$$\Delta Q_y = \frac{t}{4}\sqrt{\sum_{\{i\}} \frac{\sigma_i^2}{n y_i^2}} \quad \{i\} = 2,3,8,9$$

Here the value of t is taken from the 'Student t' table. For 95% confidence limit and infinite degree of freedom, t = 1.96.

Since σ is usually small compared to the time difference,

$$\left|\Delta K_x'\right| = \Delta Q_x / Q_x^2$$

$$\left|\Delta K_y'\right| = \Delta Q_y / Q_y^2$$

where the errors in the characteristic velocities, $\Delta K_x'$ and $\Delta K_y'$ also correspond to a 95% confidence limit.

In general $\Delta K_x'$ and $\Delta K_y'$ thus calculated are not useful in estimating a standard deviation for K because point to point scatter in ΔK cannot be smoothed over the large variations of $\Delta K_x'$ and $\Delta K_y'$ during a flight $\left(\text{speed of sound} \leq \left|\begin{matrix} K_x \\ K_y \end{matrix}\right| \leq \infty\right)$.

$\Delta K_x'/K_x^2$ and $\Delta K_y'/K_y^2$ however exhibit more reasonable behavior. This could be expected since these quantities are proportional to ΔQ_x and ΔQ_y respectively.

A plot of $\Delta K_x'/K_x^2$ is shown in Figure 2 and it is evident that these quantities can be averaged meaningfully to give an estimate of the error in characteristic velocity.

The characteristic velocity error is then

$$\Delta K_x = \left(\Delta K_x'/K_x^2\right)_{avg} K_x^2$$

$$\Delta K_y = \left(\Delta K_y'/K_y^2\right)_{avg} K_y^2$$

Since wind errors are linearly related to the errors in characterisitc velocity[3], ΔK_x and ΔK_y as calculated above give ΔW_x and ΔW_y with the same confidence limit.

A standard wind profile using 10 sec. data input interval is calculated. Figure 3 shows such a profile for SA-9. It has been found that the errors in the jth layer winds caused by errors in the (j-1)st layer are nearly equal in magnitude and opposite in direction[1]. These errors become negligible very rapidly in higher layers and are definitely ignorable after 4 layers. The errors ΔK_x and ΔK_y as calculated above are introduced at every fourth data point by replacing K_x by $K_x + \Delta K_x$ etc. and calculating the new wind profile. Its departure from the standard profile gives the wind error profile. In general the two components ΔW_x and ΔW_y are not quite equal. Their average value, $\Delta W'$ is taken. Moreover, to account for errors in the jth layer winds due to errors in the (j-1)st layer this value must be multiplied by $\sqrt{2}$. Figure 4 shows wind error and layer thickness as a function of altitude using 10 second data input intervals for SA-9.

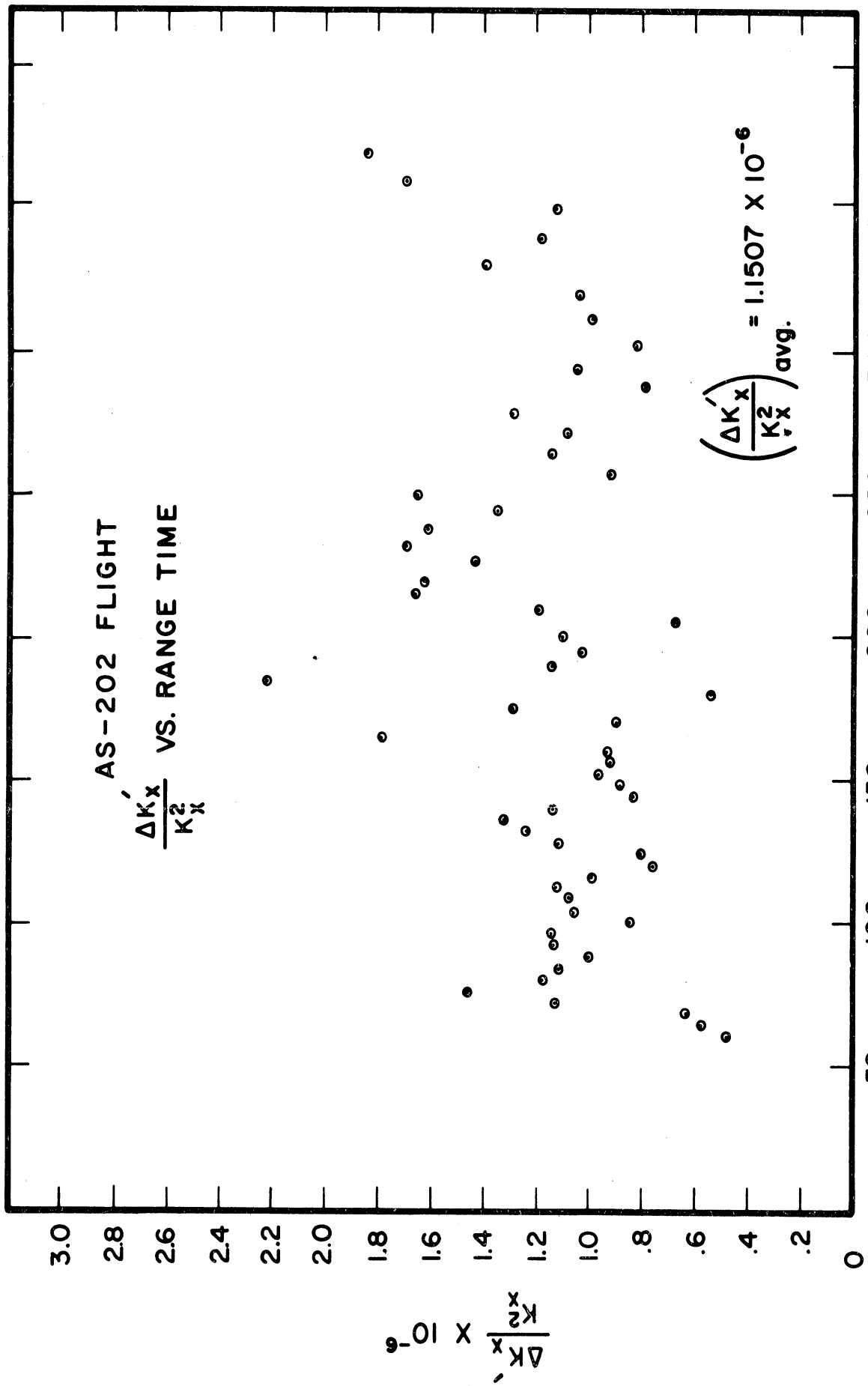
AS-202 FLIGHT
$\frac{\Delta K'_x}{K'^2_x}$ VS. RANGE TIME
$\left(\frac{\Delta K'_x}{K'^2_x}\right)_{avg.} = 1.1507 \times 10^{-6}$
$\frac{\Delta K'_x}{K'^2_x} \times 10^{-6}$
0
.2
.4
.6
.8
1.0
1.2
1.4
1.6
1.8
2.0
2.2
2.4
2.6
2.8
3.0
50
100
150
200
250
300
350
400
RANGE TIME, SEC.

FIG. 2

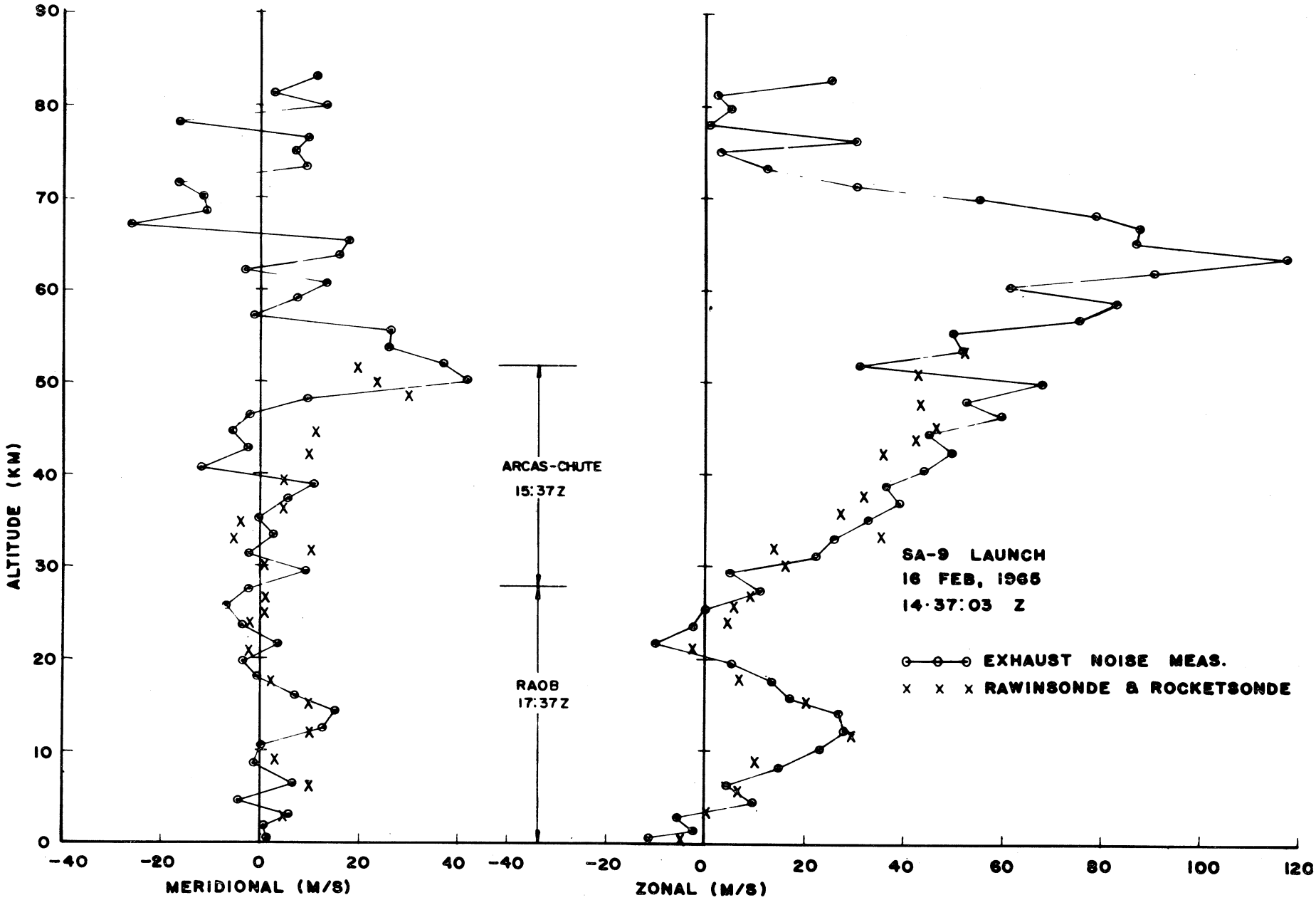

FIG. 3 SA-9 WIND PROFILE

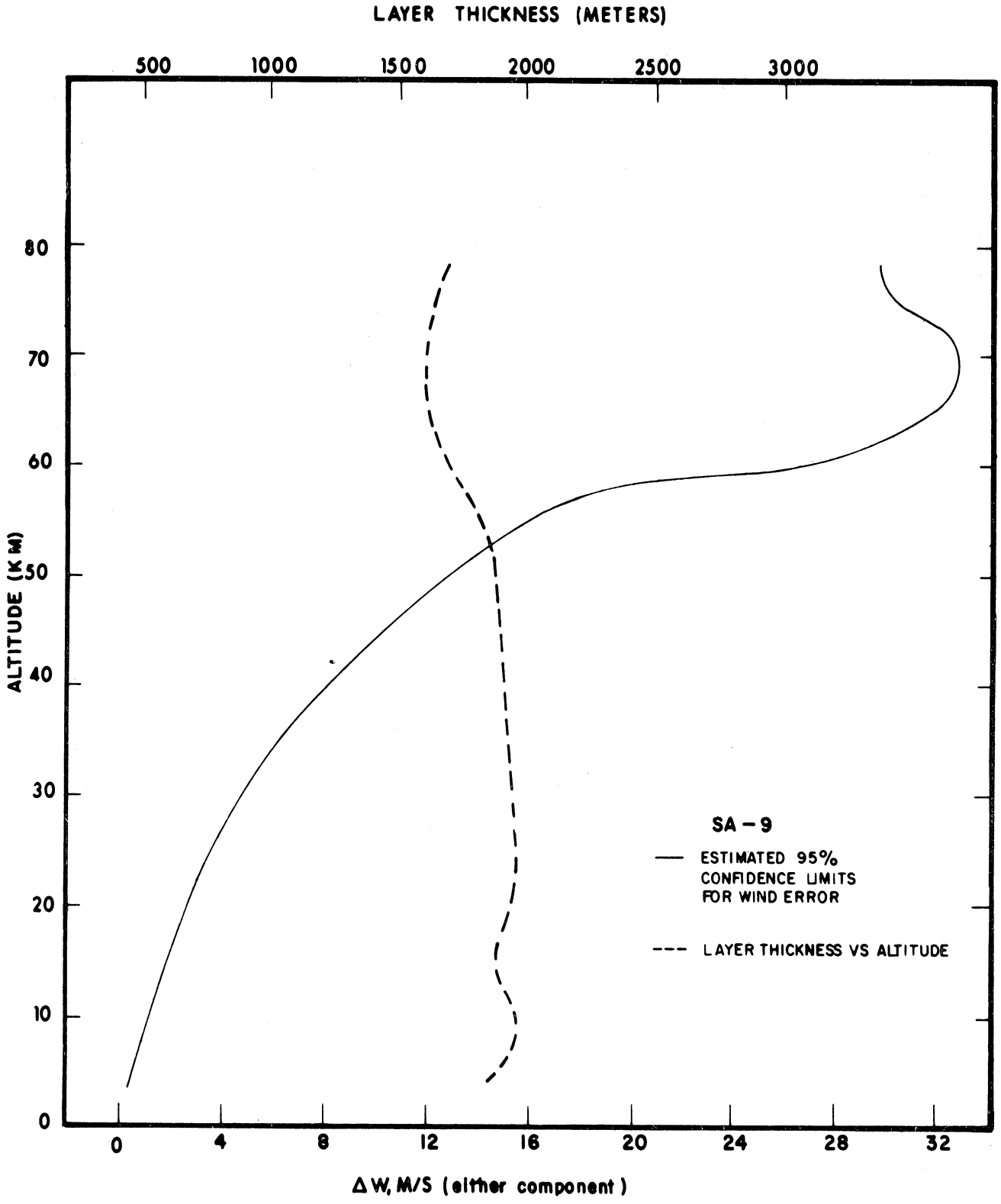
LAYER THICKNESS (METERS)
500
1000
1500
2000
2500
3000
80
70
60
50
40
30
20
10
0
ALTITUDE (KM)
0
4
8
12
16
20
24
28
32
ΔW, M/S (either component)
SA-9
ESTIMATED 95% CONFIDENCE LIMITS FOR WIND ERROR
LAYER THICKNESS VS ALTITUDE

FIG. 4

In general wind errors determined by analyzing data at 10 second intervals are large at high altitudes and small at lower altitudes. A reciprocal relation exists between layer thickness and wind errors, i.e. if layer thickness is increased, wind errors are decreased. At lower altitudes data is read in more frequently and resolution is improved. At higher altitudes, however, frequency of the input data is decreased to reduce the wind errors.

From the graph of wind error vs. altitude using 10 second data input intervals, an estimate of the layer thickness-wind error relationship can be made. From this, new wind profiles are derived that have resolution consistent with specified wind errors.

RESULTS

The wind profiles presented in Reference 2 have been modified. The new wind profiles along with wind profile errors are given here. They were generated by selecting noise events at 3 to 20 second intervals of range time resulting in wind data points separated by 500 to 2000 meters.

SA-9 Winds are measured up to the first stage burnout which occured near 85 Km. Analyzing data at 10 second intervals yielded the wind profile shown in Figure 3 and the layer thickness-error profile shown in Figure 4. To obtain a wind profile with more uniform errors at all altitudes (arbitrarily ≈ 10 m/s at 95% confidence level) the resolution was increased below 45 km and decreased above 45 km giving the error profile shown in Figure 6. The corresponding wind profile is shown in Figure 5.

Ranger-8 An anomaly in the recorded time code made these data unsuitable for computer reduction. Instead, manually read data from the oscillographs were used to derive winds up to 45 km by using data at 10 second intervals as shown in Figure 7. An error analysis was not possible for this flight.

SA-8 Three of the nine microphones were not operative during this flight. The effect of this lack of redundancy can be seen in the layer thickness-error profile graph (Figure 9) which shows higher errors and less resolution than in SA-9. In other respects which might affect the measurement, i.e. launch site, firing direction, ground winds, etc., these two flights were similar. Figure 8 shows the wind profile for this flight.

SA-10 Recorded microphone data appeared to be normal up to T + 400 seconds. From T + 400 seconds to T + 450 seconds, the oscillograph record showed the exhaust noise seemed to suffer unusually large attenuation. Because of the poor quality of the data in this section it was decided to reduce the wind errors by averaging the microphone data over 30 seconds instead of about 20 seconds which would have been normal otherwise. Figure 10 shows SA-10 wind profile and Figure 11 gives wind errors.

AS-201, AS-202, and AS-203 The first stage of the AS-Series burned out at altitudes near 60 km. The low signal to noise ratio recorded for the record stage made it impossible to use the data for wind determination. Figures 12 - 17 show the wind and error profiles for these flights. In the case of AS-203, only five of the nine microphones were operative during the flight. Just prior to this flight, four microphones were damaged as a result of their exposure to the rain. Moisture between the high voltage side of the nickle filament and element case allowed electrolysis of the filament which eventually decomposed. Again the lack of redundancy caused the layer thickness-wind error profile (Figure 17) to be less favorable than other flights.

Titan-IIIC Titan-IIIC was destroyed at an altitude of about 25 km, so no exhaust noise measurements were possible above this altitude. (Figures 18 and 19)

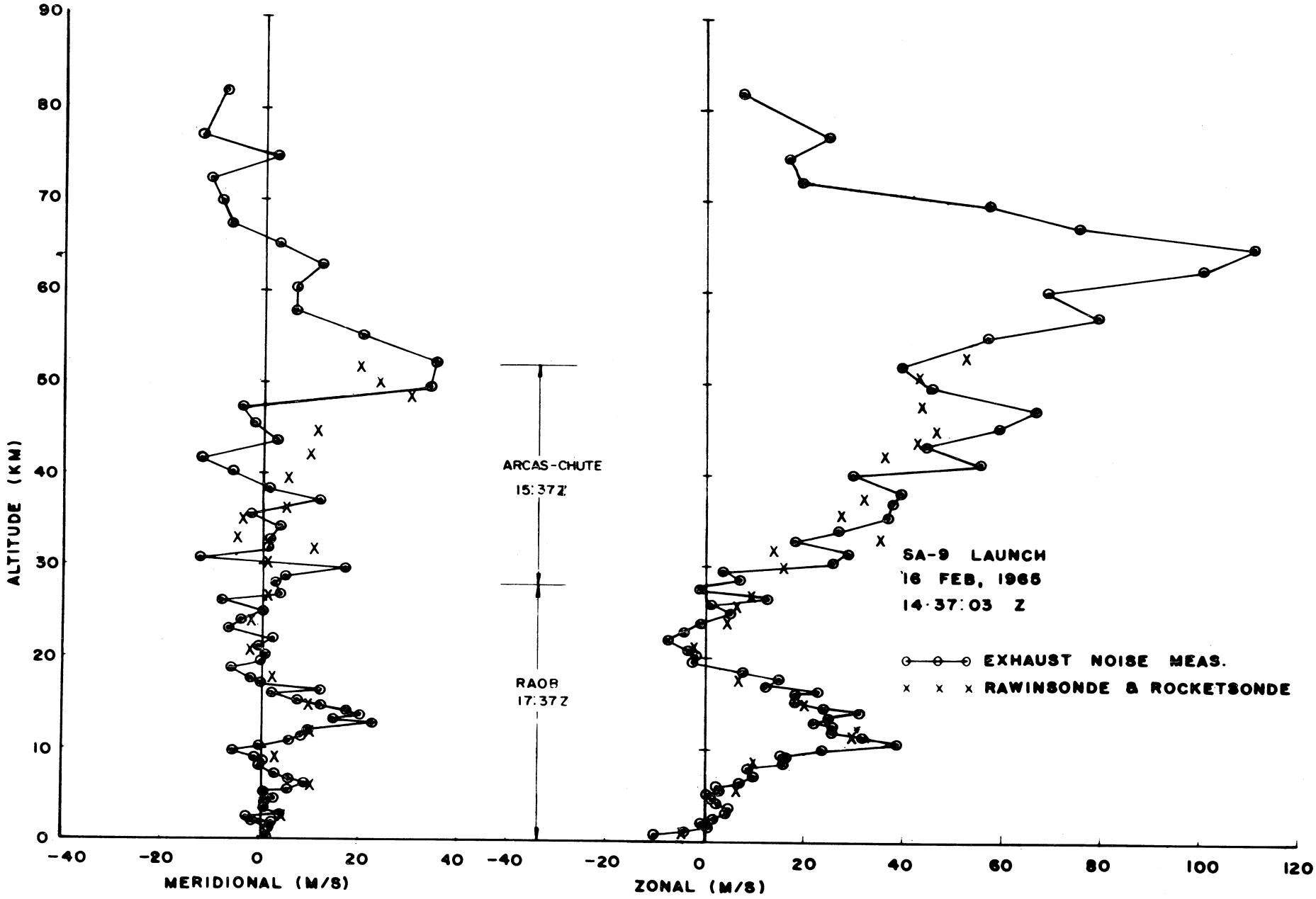
ALTITUDE (KM)
90
80
70
60
50
40
30
20
10
0
-40
-20
0
20
40
MERIDIONAL (M/S)
ARCAS-CHUTE
15:37Z
RAOB
17:37Z
-40
-20
0
20
40
60
80
100
120
ZONAL (M/S)
SA-9 LAUNCH
16 FEB, 1965
14:37:03 Z
EXHAUST NOISE MEAS.
RAWINSONDE & ROCKETSONDE

FIG. 5

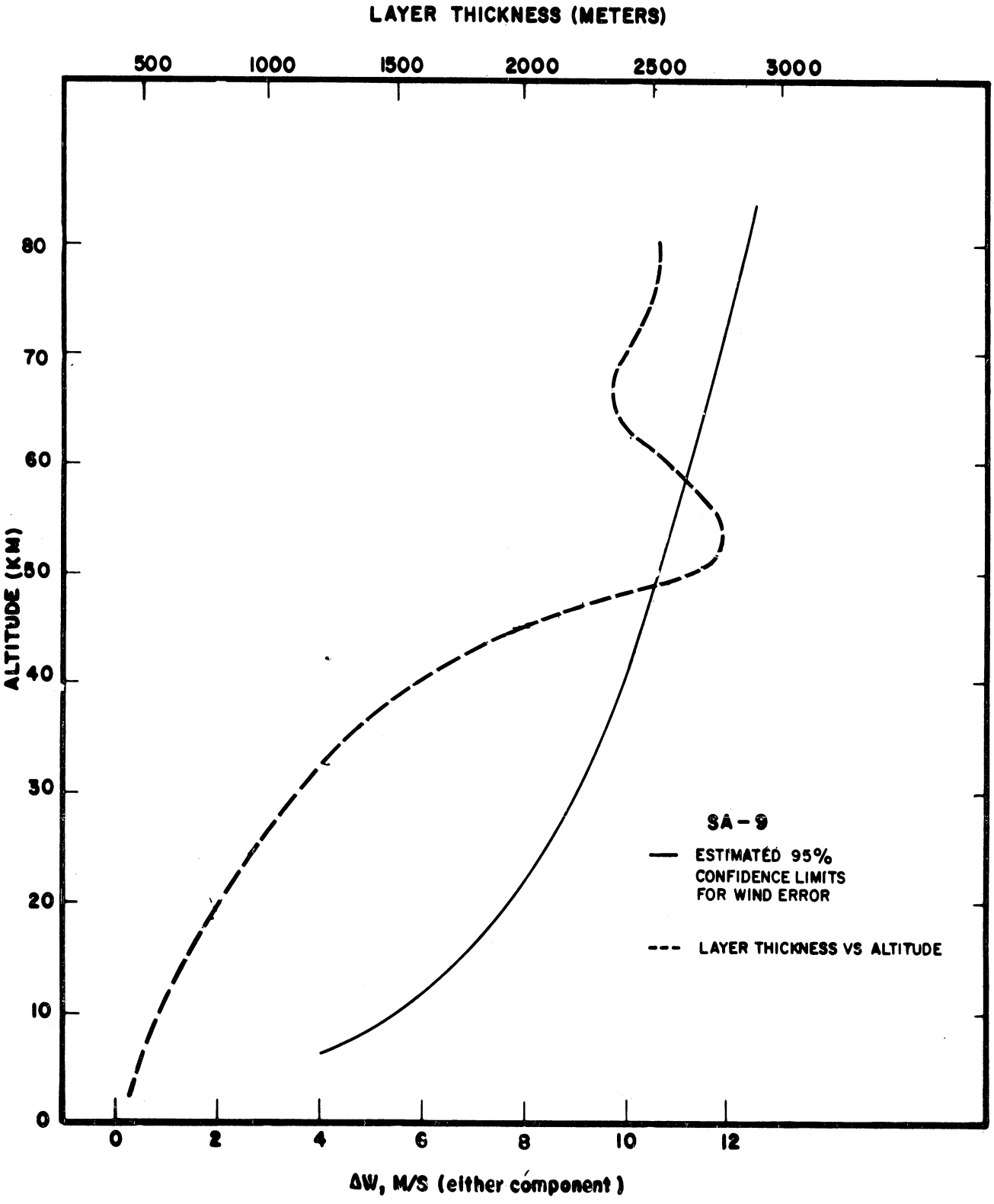
LAYER THICKNESS (METERS)
500
1000
1500
2000
2500
3000
80
70
60
50
40
30
20
10
0
ALTITUDE (KM)
0
2
4
6
8
10
12
ΔW, M/S (either component)
SA-9
ESTIMATED 95% CONFIDENCE LIMITS FOR WIND ERROR
LAYER THICKNESS VS ALTITUDE

FIG. 6

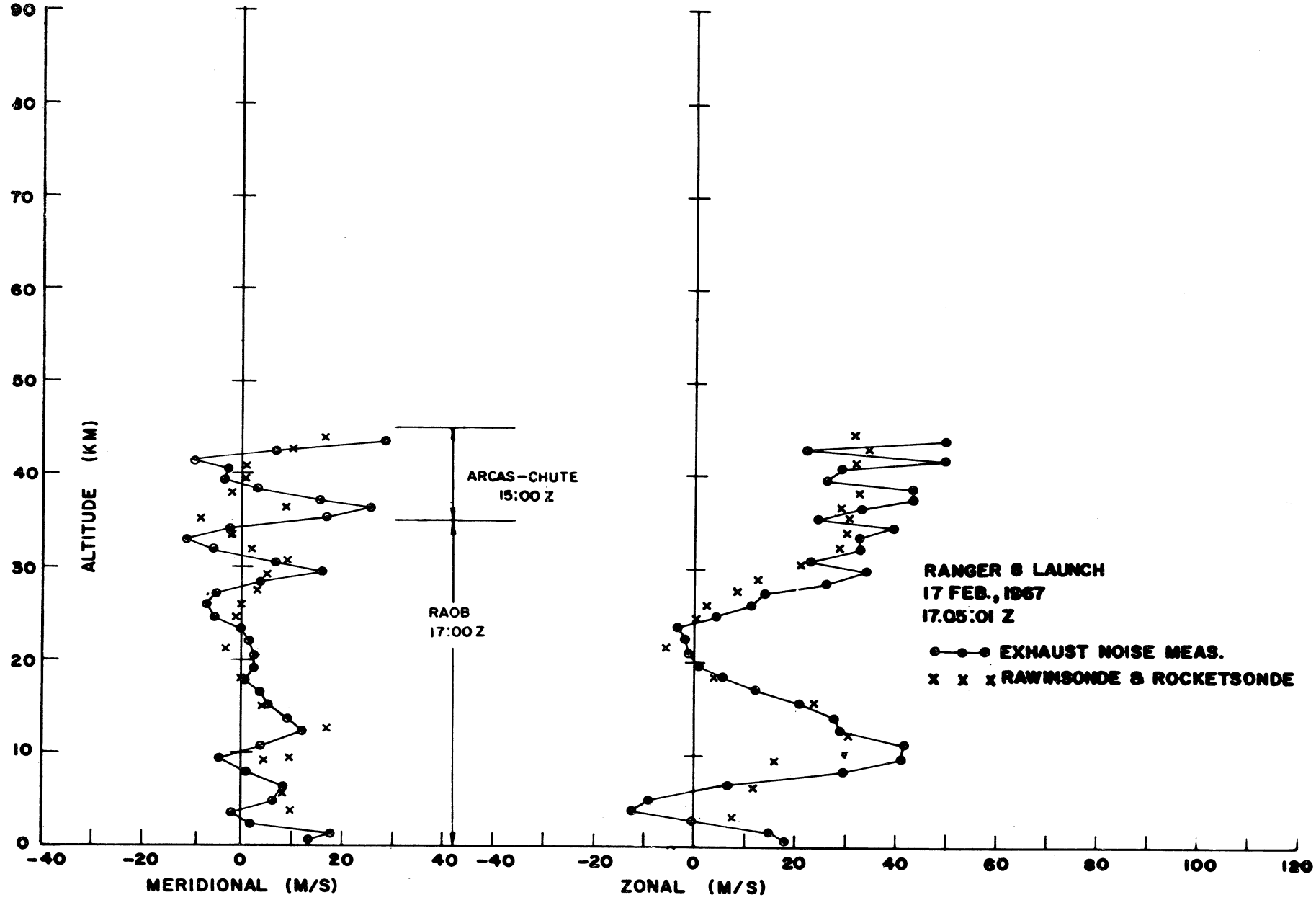
ALTITUDE (KM)
90
80
70
60
50
40
30
20
10
0
-40
-20
0
20
40
MERIDIONAL (M/S)
ARCAS-CHUTE
15:00 Z
RAOB
17:00 Z
-40
-20
0
20
40
60
80
100
120
ZONAL (M/S)
RANGER 8 LAUNCH
17 FEB., 1967
17:05:01 Z
EXHAUST NOISE MEAS.
RAWINSONDE & ROCKETSONDE

FIG. 7

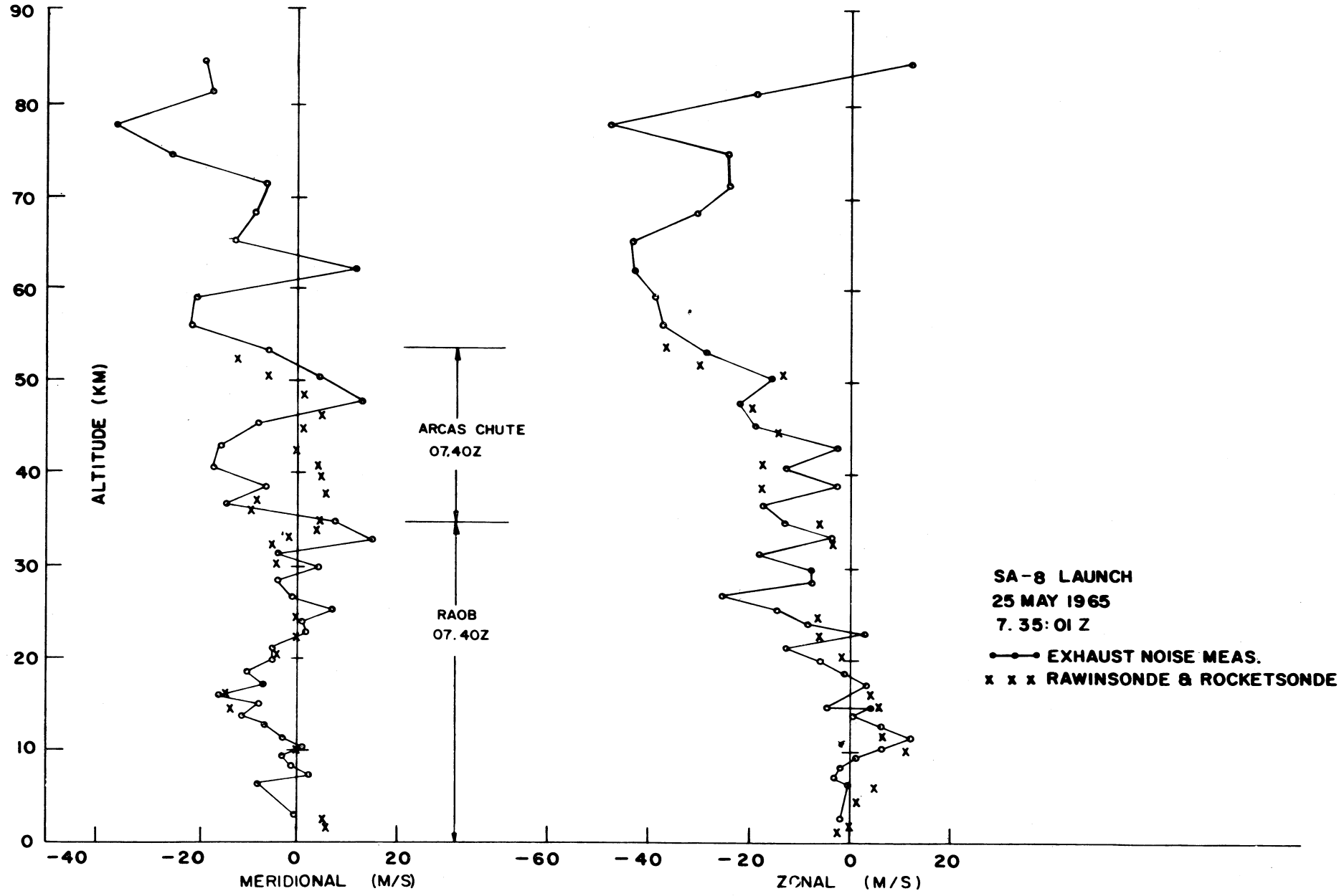
ALTITUDE (KM)
90
80
70
60
50
40
30
20
10
0
-40
-20
0
20
MERIDIONAL (M/S)
ARCAS CHUTE
07.40Z
RAOB
07.40Z
-60
-40
-20
0
20
ZONAL (M/S)
SA-8 LAUNCH
25 MAY 1965
7.35:01 Z
EXHAUST NOISE MEAS.
RAWINSONDE & ROCKETSONDE

FIG. 8

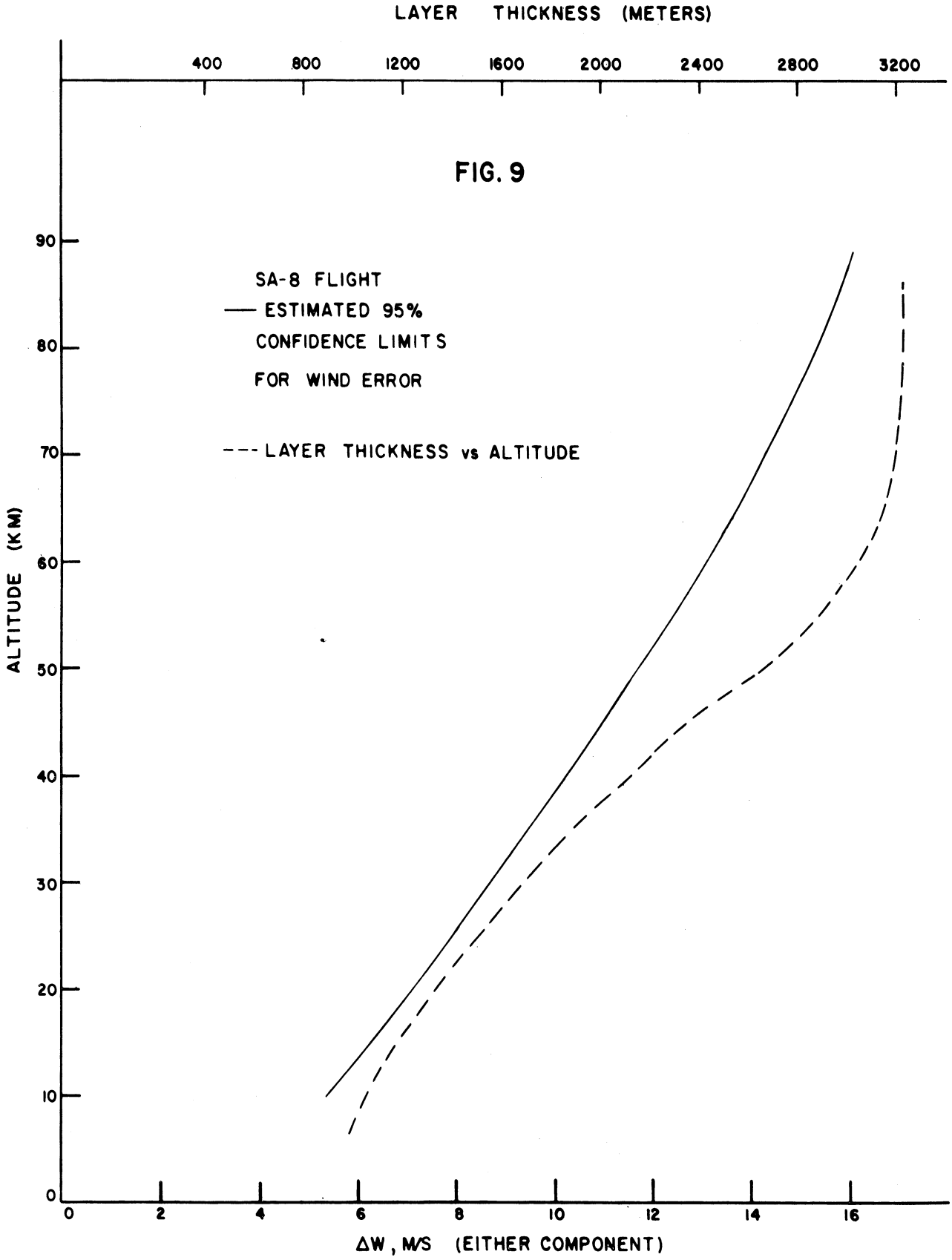
LAYER THICKNESS (METERS)
400
800
1200
1600
2000
2400
2800
3200
SA-8 FLIGHT
— ESTIMATED 95%
CONFIDENCE LIMITS
FOR WIND ERROR
--- LAYER THICKNESS vs ALTITUDE
ALTITUDE (KM)
90
80
70
60
50
40
30
20
10
0
0
2
4
6
8
10
12
14
16
ΔW, M/S (EITHER COMPONENT)

FIG. 9

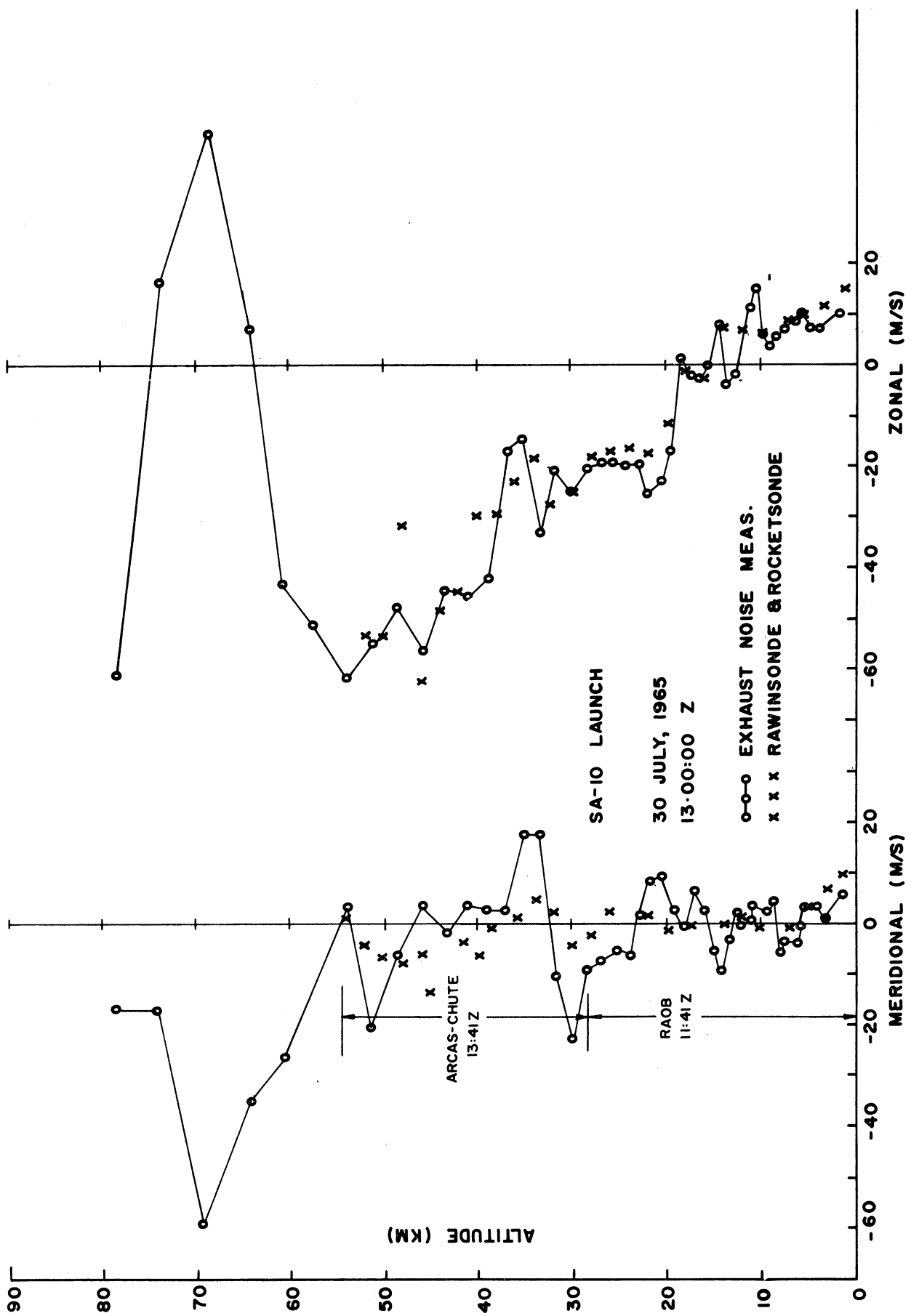
ALTITUDE (KM)
MERIDIONAL (M/S)
ZONAL (M/S)
SA-10 LAUNCH
30 JULY, 1965
13:00:00 Z
o—o—o EXHAUST NOISE MEAS.
x x x RAWINSONDE & ROCKETSONDE
ARCAS-CHUTE
13:41Z
RAOB
11:41Z

FIG. 10

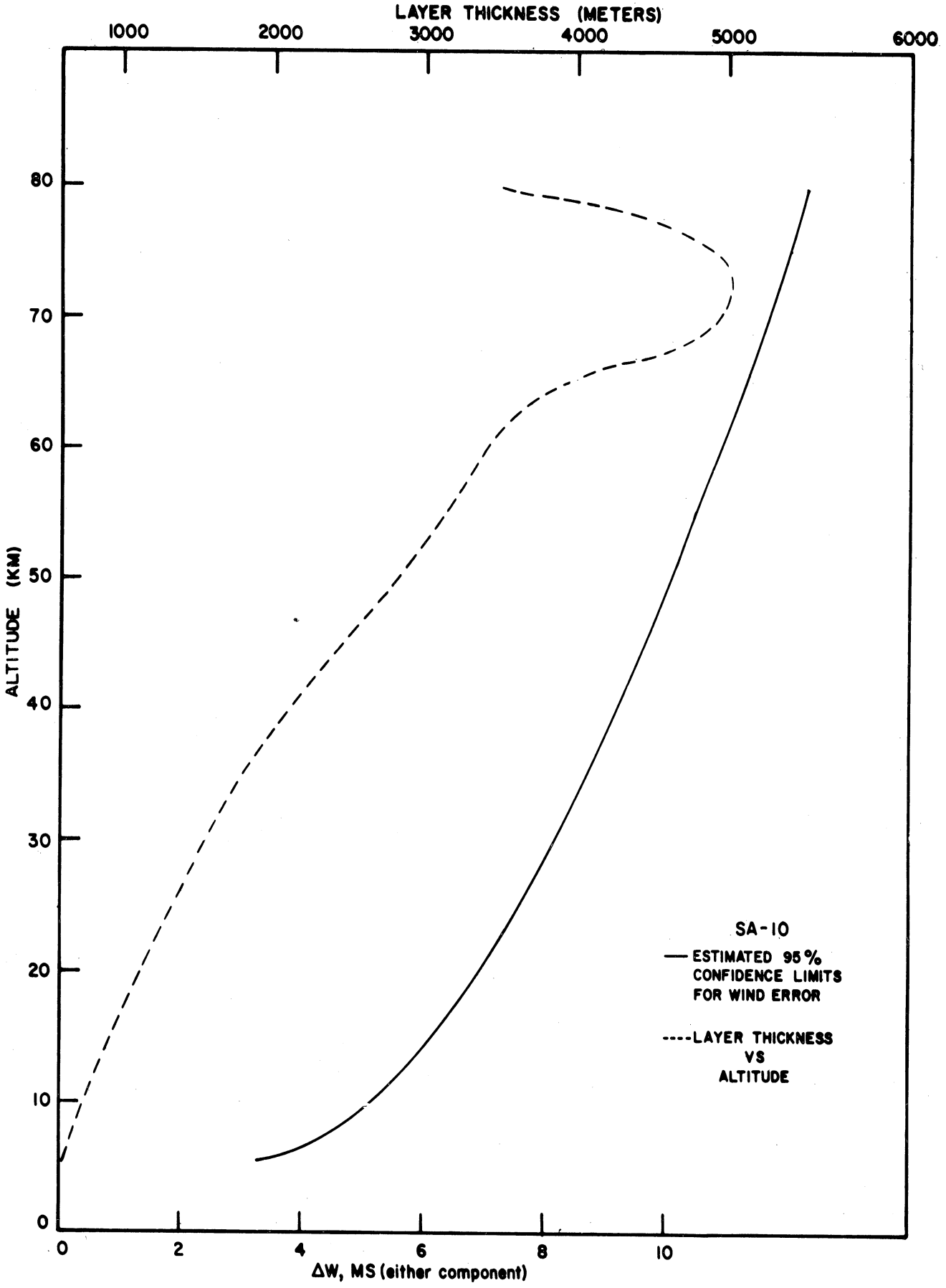
LAYER THICKNESS (METERS)
1000
2000
3000
4000
5000
6000
80
70
60
50
40
30
20
10
0
ALTITUDE (KM)
0
2
4
6
8
10
ΔW, MS (either component)
SA-10
— ESTIMATED 95% CONFIDENCE LIMITS FOR WIND ERROR
----LAYER THICKNESS VS ALTITUDE

FIG. 11

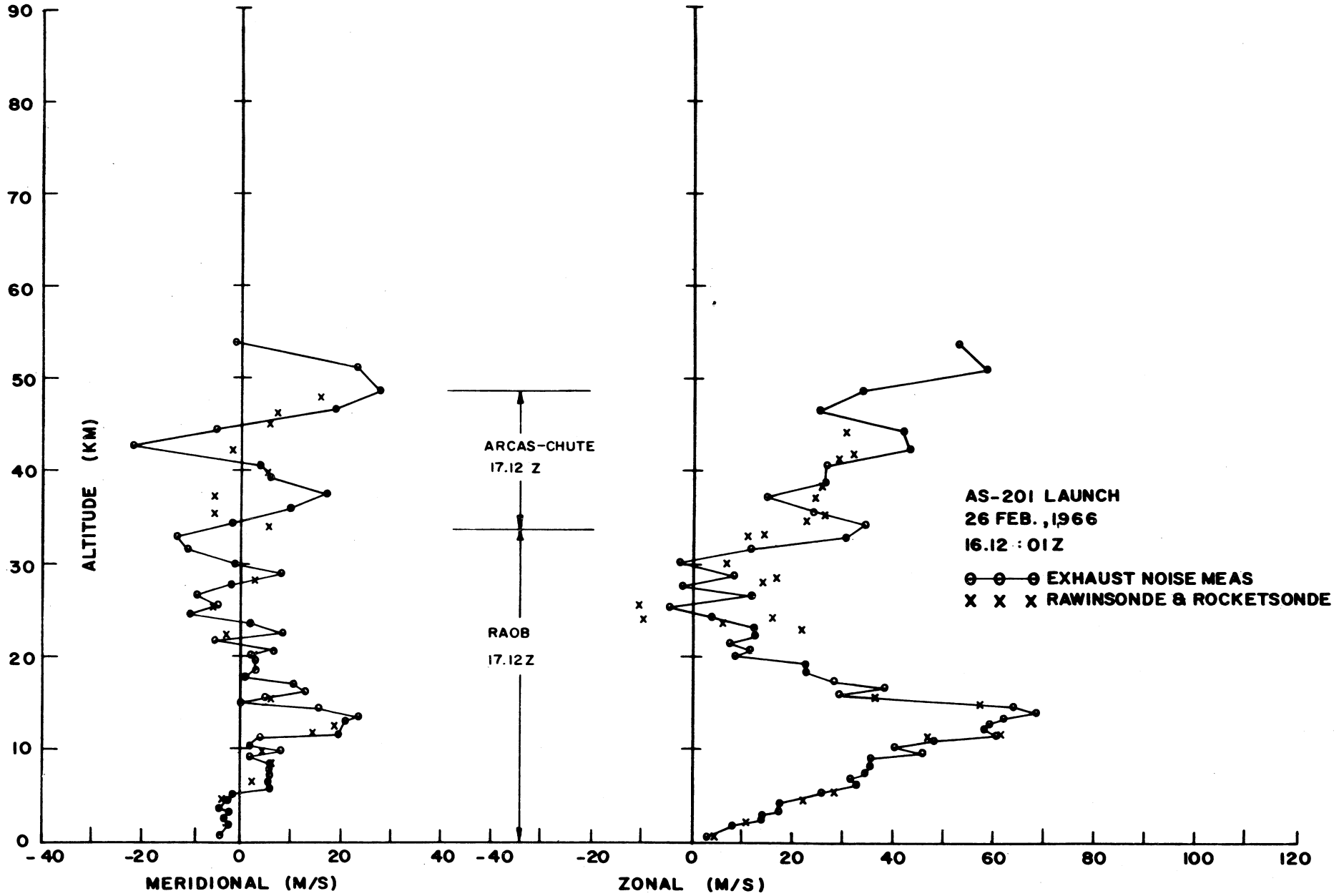
ALTITUDE (KM)
MERIDIONAL (M/S)
ZONAL (M/S)
ARCAS-CHUTE
17.12 Z
RAOB
17.12Z
AS-201 LAUNCH
26 FEB., 1966
16.12 : 01Z
EXHAUST NOISE MEAS
RAWINSONDE & ROCKETSONDE

FIG 12

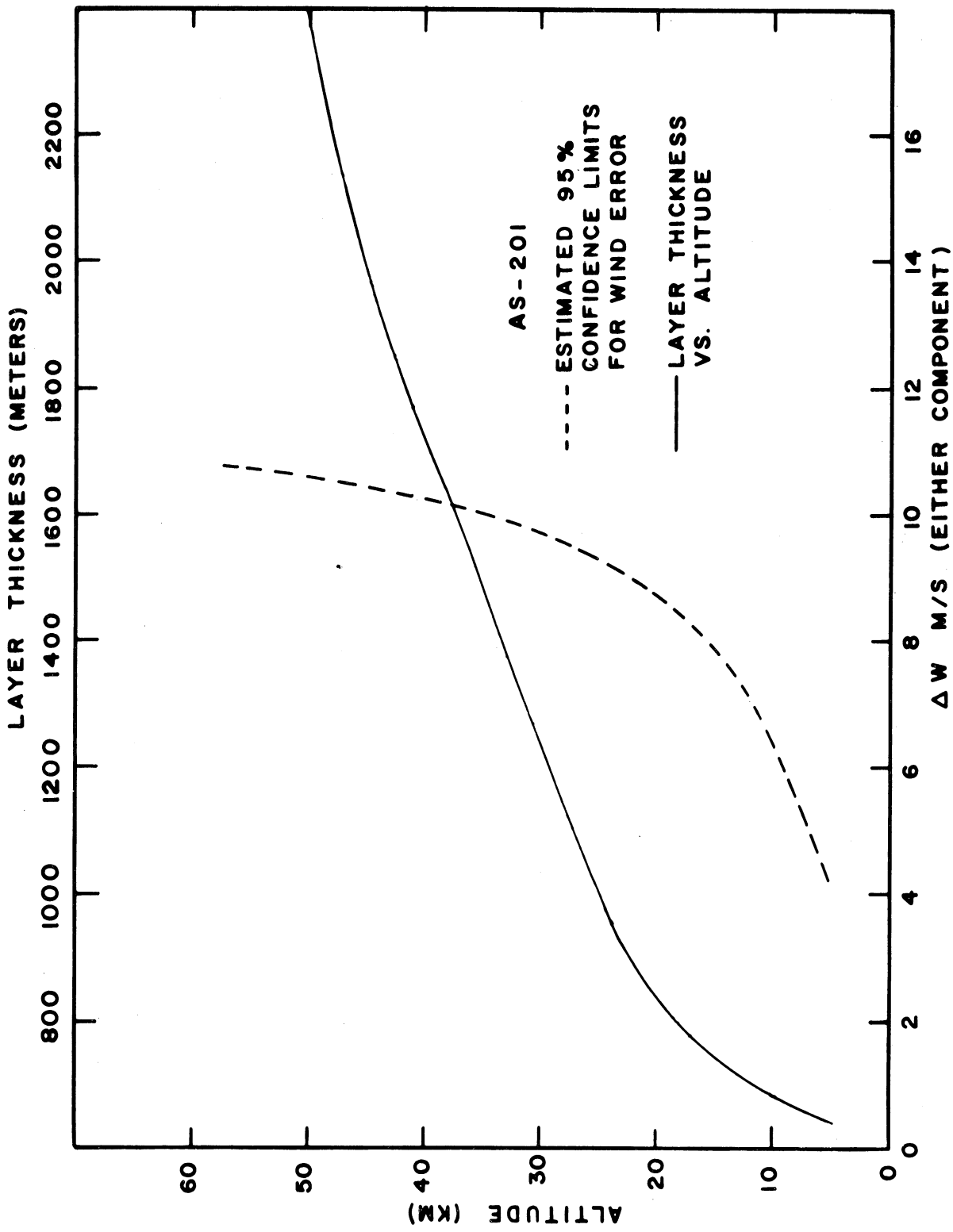
LAYER THICKNESS (METERS)
800
1000
1200
1400
1600
1800
2000
2200
ALTITUDE (KM)
60
50
40
30
20
10
0
ΔW M/S (EITHER COMPONENT)
0
2
4
6
8
10
12
14
16
AS-201
---- ESTIMATED 95% CONFIDENCE LIMITS FOR WIND ERROR
—— LAYER THICKNESS VS. ALTITUDE

FIG. 13

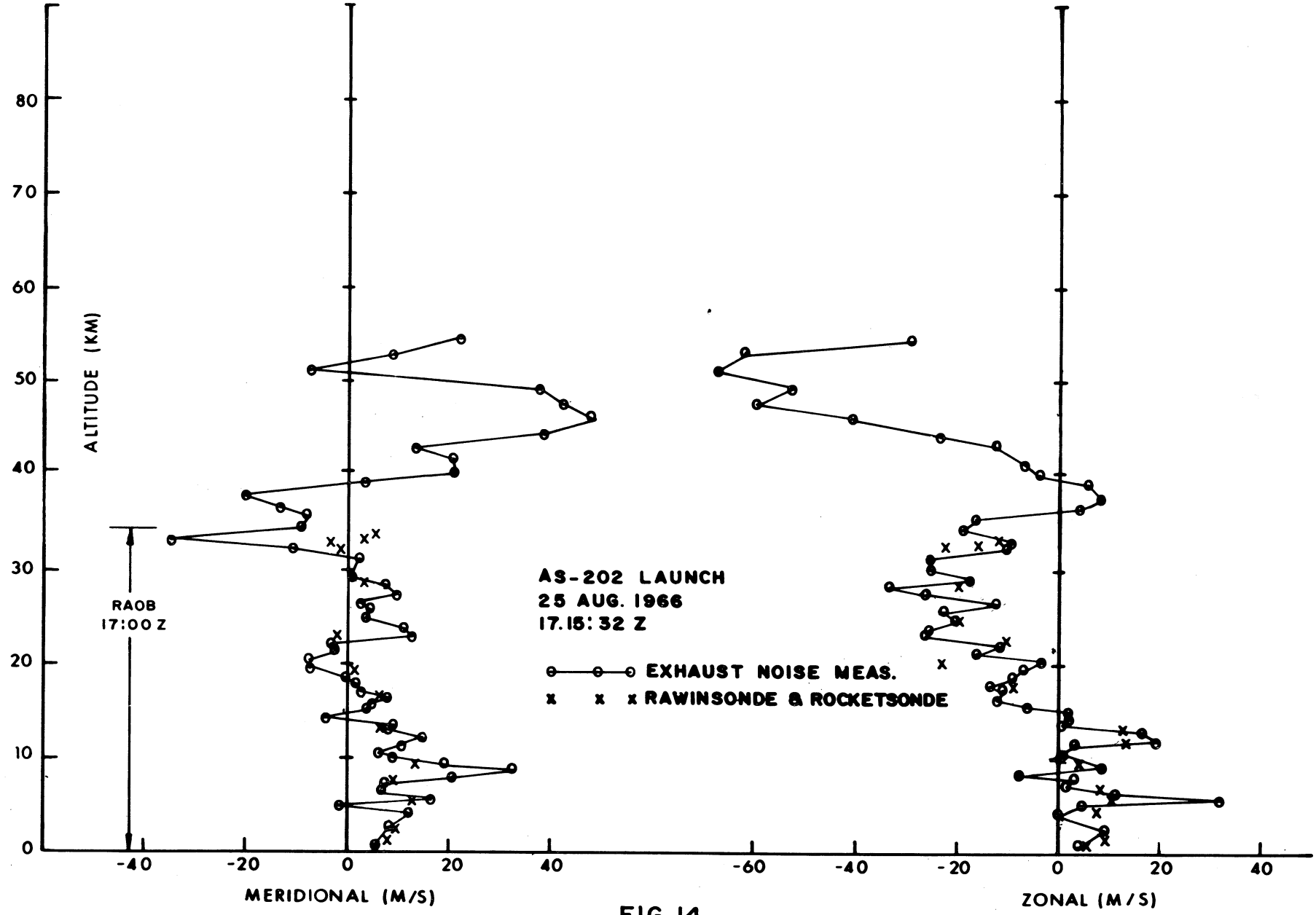
ALTITUDE (KM)
80
70
60
50
40
30
20
10
0
RAOB
17:00 Z
AS-202 LAUNCH
25 AUG. 1966
17.15:32 Z
EXHAUST NOISE MEAS.
RAWINSONDE & ROCKETSONDE
-40
-20
0
20
40
MERIDIONAL (M/S)
-60
-40
-20
0
20
40
ZONAL (M/S)

FIG. 14

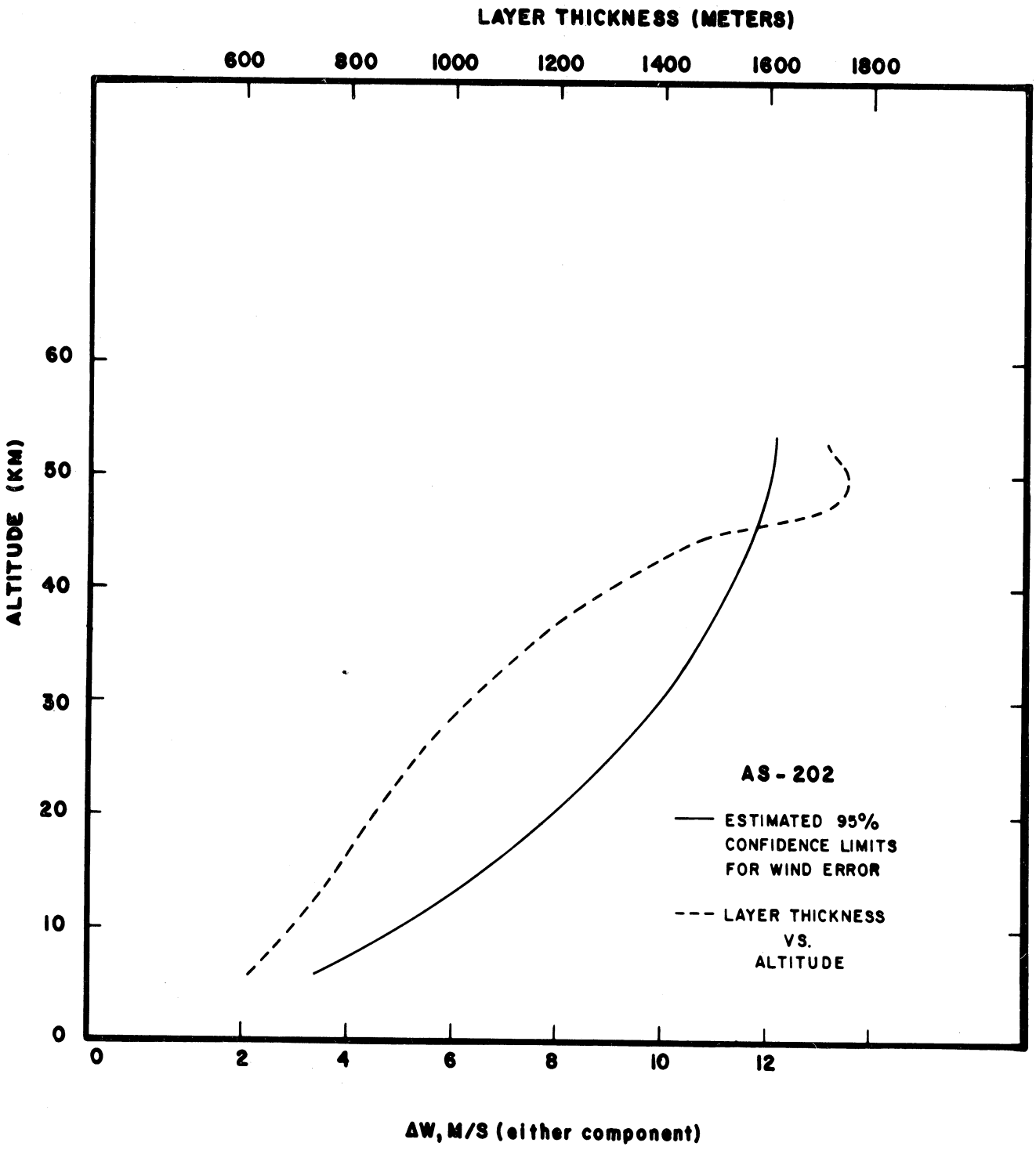
LAYER THICKNESS (METERS)
600
800
1000
1200
1400
1600
1800
ALTITUDE (KM)
60
50
40
30
20
10
0
0
2
4
6
8
10
12
ΔW, M/S (either component)
AS-202
ESTIMATED 95% CONFIDENCE LIMITS FOR WIND ERROR
LAYER THICKNESS VS. ALTITUDE

FIG. 15

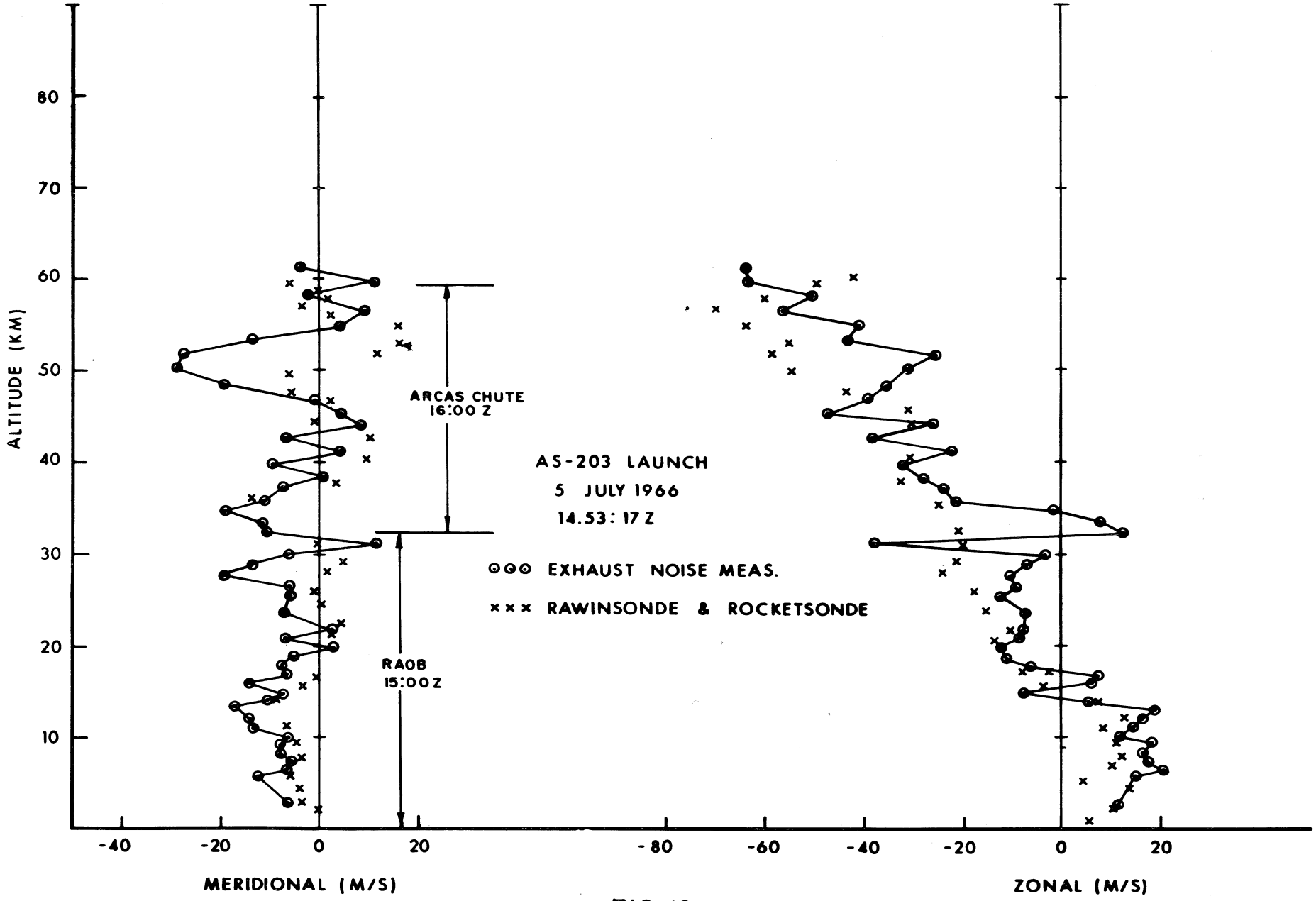
ALTITUDE (KM)
80
70
60
50
40
30
20
10
ARCAS CHUTE
16:00 Z
RAOB
15:00 Z
AS-203 LAUNCH
5 JULY 1966
14.53: 17 Z
⊙⊙⊙ EXHAUST NOISE MEAS.
××× RAWINSONDE & ROCKETSONDE
-40
-20
0
20
MERIDIONAL (M/S)
-80
-60
-40
-20
0
20
ZONAL (M/S)

FIG. 16

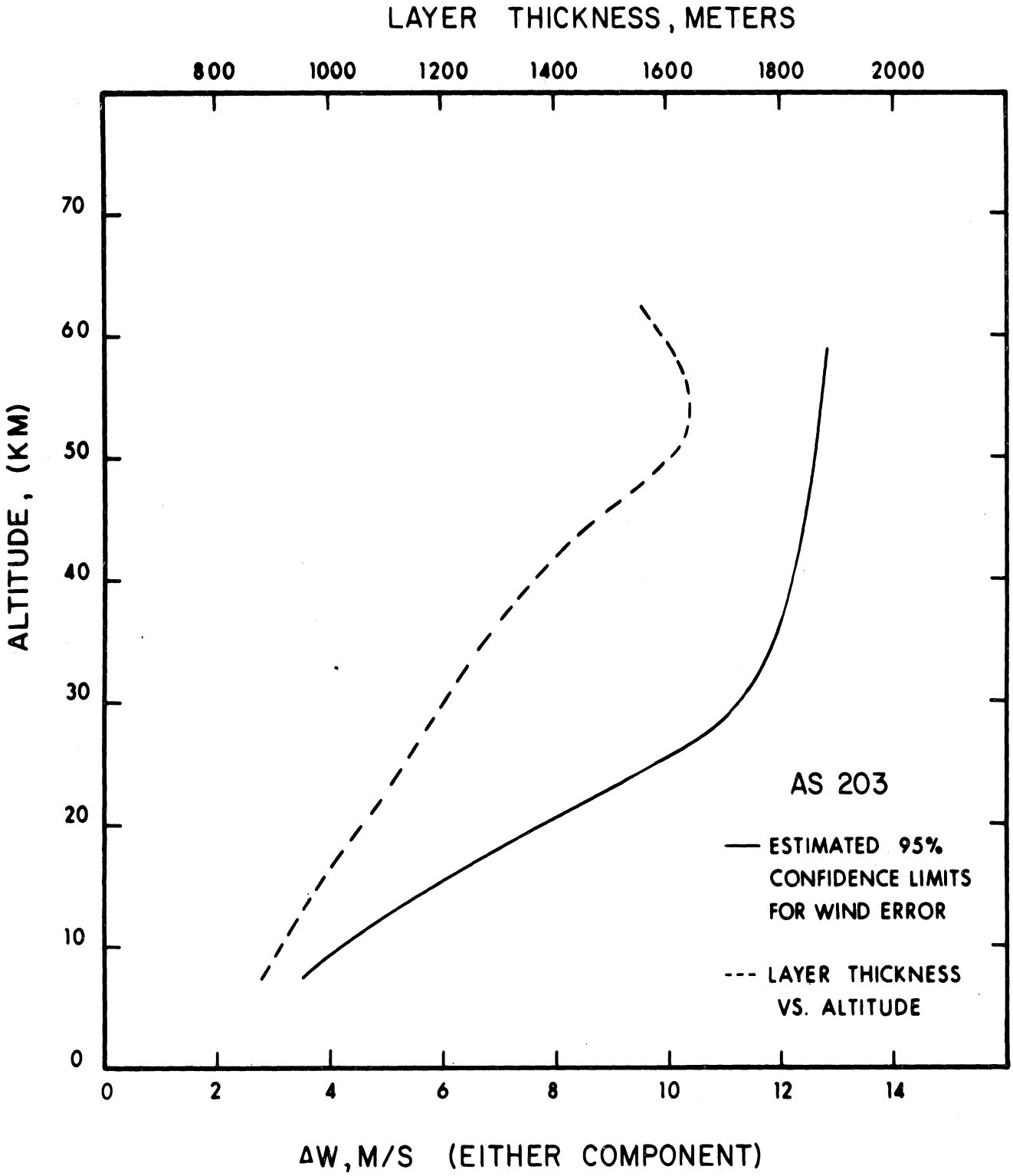
LAYER THICKNESS, METERS
800
1000
1200
1400
1600
1800
2000
ALTITUDE, (KM)
70
60
50
40
30
20
10
0
0
2
4
6
8
10
12
14
ΔW, M/S (EITHER COMPONENT)
AS 203
— ESTIMATED 95% CONFIDENCE LIMITS FOR WIND ERROR
--- LAYER THICKNESS VS. ALTITUDE

FIG. 17

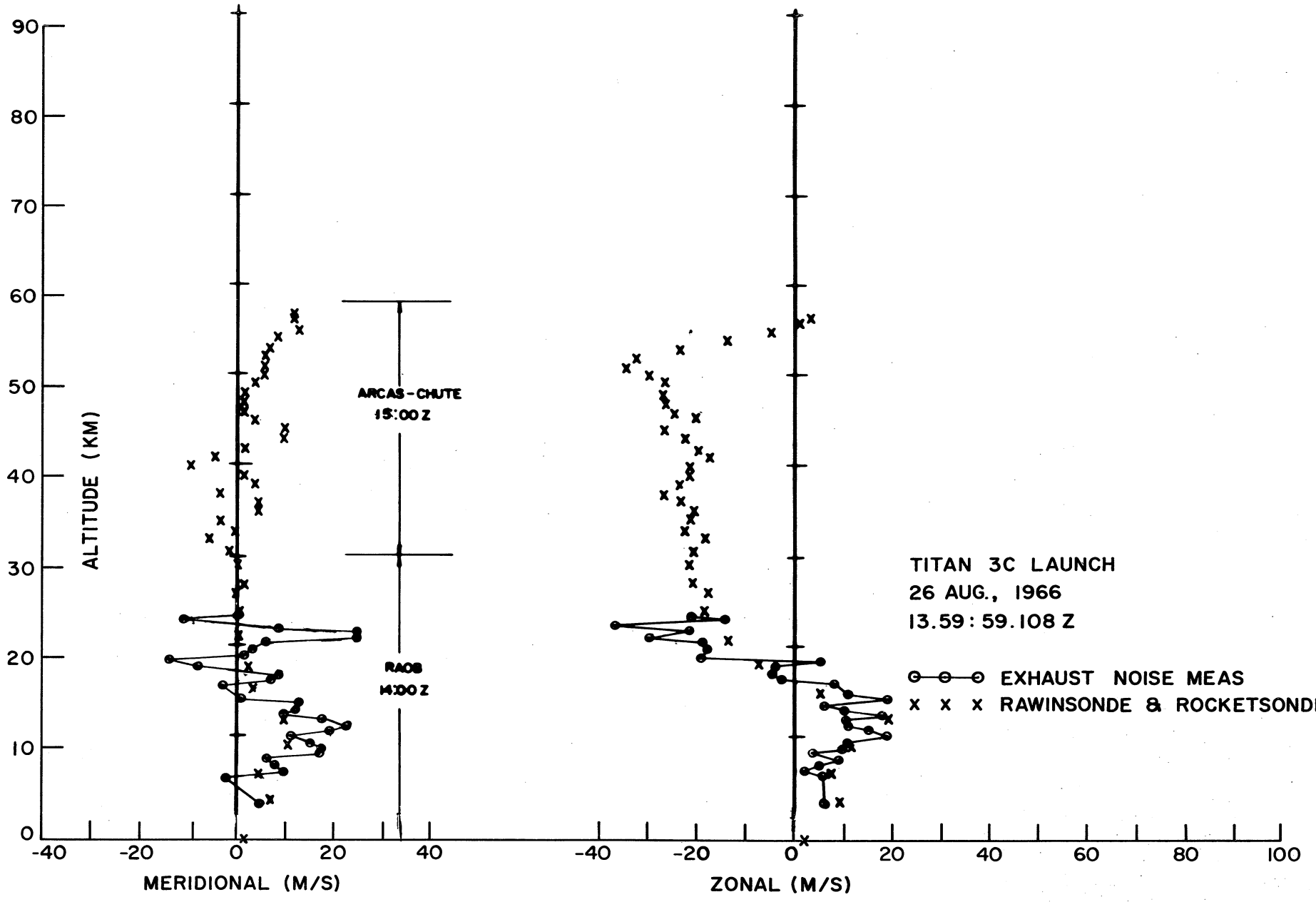
ALTITUDE (KM)
90
80
70
60
50
40
30
20
10
0
ARCAS-CHUTE
15:00 Z
RAOB
14:00 Z
-40
-20
0
20
40
MERIDIONAL (M/S)
-40
-20
0
20
40
60
80
100
ZONAL (M/S)
TITAN 3C LAUNCH
26 AUG., 1966
13.59:59.108 Z
EXHAUST NOISE MEAS
RAWINSONDE & ROCKETSONDE

FIG. 18

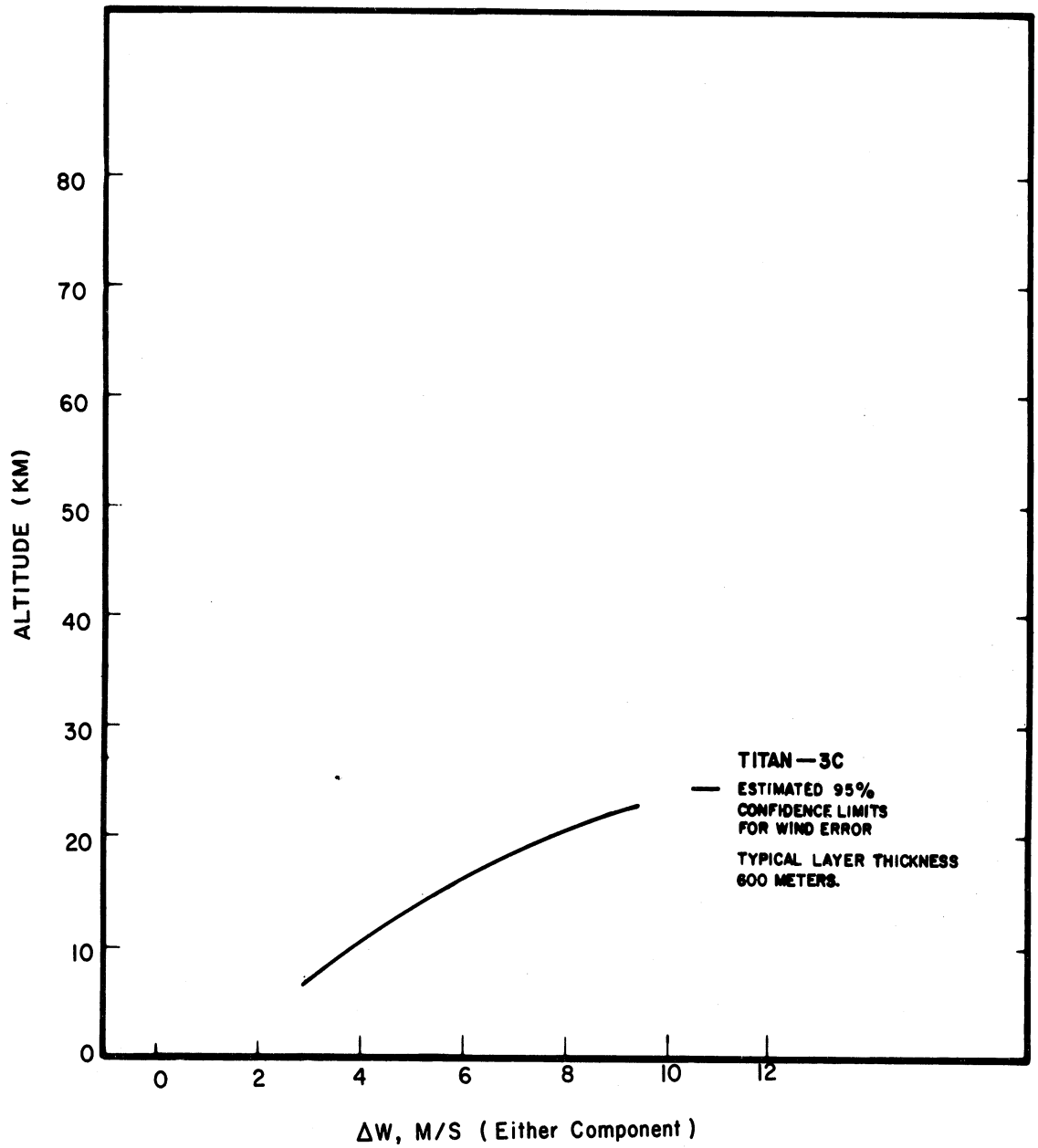
ALTITUDE (KM)
80
70
60
50
40
30
20
10
0
0
2
4
6
8
10
12
ΔW, M/S (Either Component)
TITAN—3C
ESTIMATED 95%
CONFIDENCE LIMITS
FOR WIND ERROR
TYPICAL LAYER THICKNESS
600 METERS.

FIG. 19

REFERENCES

1. Bushman, W. W., G. M. Kakli, and G. R. Carignan, An Acoustic Wind Measuring Technique. University of Michigan, Space Physics Research Laboratory, Technical Report 05911-2-T, Contract NAS8-11054, July 1965.

2. Bushman, W. W., An Acoustic Wind Measurement: A Six Month Summary. University of Michigan, Space Physics Research Laboratory, Technical Report 07871-1-T, Contract NAS8-20457, September 1966.

3. Bushman, W. W., G. R. Carignan, G. M. Kakli, and O. E. Smith, High Altitude Wind Measurements from Rocket Exhaust Noise. (Submitted to J. Geophys. Res.), 1967.